Yuelong Jia[1], Li Hao[1], Zhengjun Shi[2], Haojun Zhu[2], and Jiansheng Yuan[1]

State Key Lab of Power System, Tsinghua University, China (1), Grid Planning & Research Centre, Guangdong Power Grid Corporation (2)

doi:10.15199/48.2016.04.03

Simplified Method for Computing Reactance in the Design of Saturated-Core Superconducting Fault Current Limiter

Abstract. *Generally, the computation of the steady-state reactance of the SCSFCL employs the nonlinear steel core model with both the DC and AC excitation. Noting the deep saturation region of the B-H curve is nearly a straight line, a simplified method is presented in this paper. The slope of the deep saturation region of the B-H curve is taken as an equivalent permeability for the core. Furthermore, the computation can be simplified as a static-magnetic-field model when ignoring the eddy current effect. The example shows this simplified method meets the engineering requirements.*

Streszczenie. *Obliczenia reaktancji SCSFCL wymaga użycia nieliniowego modelu rdzenia stalowego zarówno dla wzbudzenia stałoprądowego jak i zmiennoprądowego. W artykule przedstawiono uproszczoną metodę obliczania reaktancji zakładając, że w obszarze dużego nasycenia krzywa B-H jest prawie linią prostą. Jako przenikalność rdzenia przyjęto nachylenie krzywej B-H w obszarze głębokiego nasycenia. Ponadto, obliczenia mogą być uproszczone przez pominięcie prądów wirowych i przyjęcie modelu statycznego. Przykład pokazuje, że metoda uproszczona spełnia wymagania inżynierskie* ***(Uproszczona metoda obliczania reaktancji w projektowaniu nadprzewodzącego ogranicznika prądu z nasyconym rdzeniem)***.

Keywords: dynamic permeability, reactance design, saturated core, superconducting fault current limiter.
Słowa kluczowe: przenikalność dynamiczna, projektowanie reaktancji, rdzeń nasycony, nadprzewodzący ogranicznik prądu

Introduction

As the power grid becomes much larger and the connection becomes much stronger, the short-circuit fault current goes up continuously, and is reaching up to and even going beyond the maximum value that the circuit breaker can cut off [1-2]. So effective means of limiting the short-circuit fault current has to be found. Traditional methods to limit the short-circuit fault current like splitting the bus bars will affect the flexibility and stability of the power grid [3-4]. Due to its characteristics, the saturated-core superconducting fault current limiter (SCSFCL) has become an important means of limiting the fault current. In the steady working state of the power grid, it has small reactance so that the normal operation of the power grid is nearly not affected, and when the short-circuit fault occurs, high voltage pulses will be induced on the SCSFCL to limit the fault current.

Although the SCSFCL has two working states, only the steady-state reactance is the fundamental indicator for the structural design, and the properties of the limiting state will not be taken into consideration in the structure design process. This is because the limiting-state properties are closely related to the structure of the power grid, the parameters of the power grid and the specific installation location of the SCSFCL. The limiting-state property computation for the SCSFCL installed in a specific grid needs transient simulation of the power grid [5-6], which is not concentrated in this paper. More importantly, the structural requirements for the steady state and the limiting state are just opposite to each other. When the steady-state reactance of the SCSFCL is determined, its limiting-state properties are almost fixed, without much room for optimization.

Generally, the computation for steady-state reactance must employ nonlinear models with both DC and AC excitation and has to be solved in time domain [7-8]. Such computation process consumes long calculation time and may lead to large error due to nonlinear solution process. This paper presents a simplified computation method, which converts the nonlinear time-domain problem to linear frequency-domain one by the equivalent linear permeability concept. When the eddy current effect in the laminated steel cores and the structural parts is ignored, the computation method can even be simplified as static-magnetic-field computation. The computation example is given in the end, and the result shows the simplified method meets the engineering requirements.

Introduction of working principle of the SCSFCL

A set of the SCSFCL consists of a superconducting DC coil, two copper AC coils in series with the AC power line, and two steel cores, as shown in Fig. 1. One kind of the core and coil structure is shown in Fig. 2, where the DC coil provides DC magnetic bias for the steel cores.

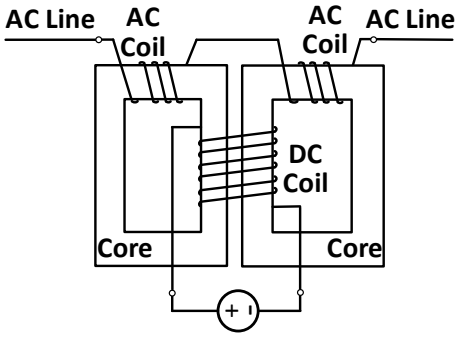

Fig.1. Principle structure of the SCSFCL.

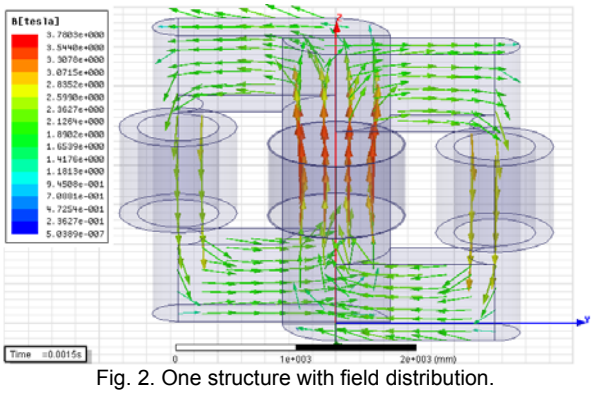

Fig. 2. One structure with field distribution.

A. Working Principle in Steady State

In the steady working state of the power grid, the large DC magnetic field intensity H_{DC} is generated in the steel cores by the large current in the superconducting DC coil. The steel cores are thus driven into deep saturation region of the *B-H* curve, as shown in Fig. 3, where the influence that the current in the AC coils has on the magnetic field in

the steel cores is denoted by H_{AC}. The behavior of the steel cores varies between P_1 and P_2 on the *B-H* curve as H_{AC} varies. Since the cores remain in the deep saturation state, however large H_{AC} is, the corresponding flux density denoted by B_{AC} varies in a relatively small range. So the induced voltage on AC coils derived from B_{AC} is also small. Consequently, considering that the value of H_{AC} corresponds to the value of the AC current, the steady-state reactance *X*, i.e., the ratio of the RMS voltage to RMS current, is small, as shown below:

$$X = \frac{U}{I}, \tag{1}$$

where *U* is the RMS voltage and *I* is the RMS current.

B. Working Principle in Limiting State

When the short-circuit fault happens in the power grid, the DC supply for the superconducting DC coil will be cut off. In periods of an AC excitation cycle, the steel cores pass the linear region of the *B-H* curve, thus inducing high voltage on the AC coils of SCSFCL, which is able to limit the fault current. As the time when the steel cores stay in the linear region with high permeability is very short compared with the whole cycle, the voltage is in pulse waveforms as shown in Fig. 4. The amplitude and the width of the pulses are affected by the structure parameters of SCSFCL. As previously mentioned, the limiting-state reactance computation of the SCSFCL in a specific power grid needs the transient simulation of the power grid, so it is beyond the research in this paper.

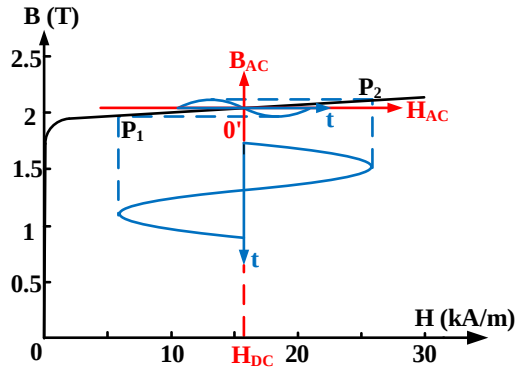

Fig. 3. *B-H* curve of the steel cores and magnetic waveforms.

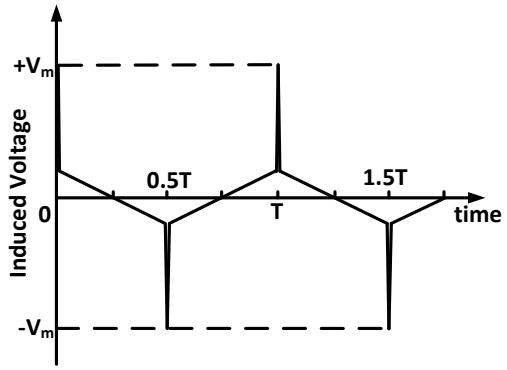

Fig. 4. Induced voltage waveform in limiting state.

Simplified method to compute steady-state reactance

The critical task for computing reactance is solving the field, as the reactance can be obtained easily afterwards.

A. Time-domain Nonlinear-Model Computation Method

Strictly speaking, the traditional nonlinear model should be employed and solved in time domain to get the magnetic field of the SCSFCL.

Under the excitation of both the DC coil and the AC coils, the steel cores work in the saturation region. So the static permeability (*B/H*) of the steel cores changes with the variation of the AC excitation. If the static permeability decreases, the ability of cores to conduct field will decrease, so that more AC leakage flux will be produced. Therefore, the field at any point inside the steel cores is not strictly in linear relation with the exciting current. Nor is H_{AC} with AC excitation. Consequently, when AC excitation is sinusoidal, H_{AC} is not strictly sinusoidal. Only time-domain nonlinear-model computation method can solve such kind of magnetic field.

However, the solving process of this method is complex, and it is not necessary to employ this theoretically complete method to compute steady-state reactance of the SCSFCL in real design process.

B. Frequency-domain Linear-Model Computation Method

Although the slope of the *B-H* curve saturation region decreases with the increase of the magnetic field intensity, the slope of the deep saturation region changes little. So the deep saturation region, like the P_1-P_2 part in Fig. 3, can be considered as a straight line. Based on this approximation, the calculation of the magnetic field can be simplified.

The magnetic field in the AC coils can be divided into two parts:

$$H(t) = H_{DC} + H_{AC}(t), \tag{2}$$

$$B(t) = B_{DC} + B_{AC}(t), \tag{3}$$

where H_{DC} and B_{DC} are magnetic field excited only by DC coil when current in the AC coils is 0, and $H_{AC}(t)$ and $B_{AC}(t)$ are the changing part when current in the AC coils is also added.

Obviously, $H_{AC}(t)$ and $B_{AC}(t)$ are key to computing the steady-state reactance. To analyze the AC magnetic field alone, the DC magnetic field is removed and an AC *B-H* curve is defined as B_{AC}-H_{AC} in the newly built coordinate system $B_{AC}0'H_{AC}$. This coordinate system is created by moving B0H until the new origin point 0' is located at the point in the *B-H* curve corresponding to H_{DC}, as shown in Fig. 3. P_1-P_2 part can then be approximately considered a straight line across origin 0'. So the relation between B_{AC} and H_{AC} becomes linear, and for AC magnetic field calculation the nonlinear problem is transferred to a linear one. The equivalent magnetic permeability is the slope of P_1-P_2 part, actually the dynamic permeability of the steel cores, and the DC excitation can be removed.

This transformation could be proved by mathematical analysis.

As the *B-H* curve can be expressed as:

$$B(t) = f[H(t)], \tag{4}$$

So take (2) and (3) into (4), we can get:

$$B_{DC} + B_{AC}(t) = f[H_{DC} + H_{AC}(t)], \tag{5}$$

Applying Taylor expansion to the right part of (5) will yield:

$$B_{DC} + B_{AC}(t) = f[H_{DC}] + f'[H_{DC}]H_{AC}(t) + \frac{f''[H_{DC}]}{2}H_{AC}^2(t) + \ldots \tag{6}$$

When there is current only in the DC coil, the magnetic field in the steel cores satisfies:

$$B_{DC} = f[H_{DC}], \tag{7}$$

And as the deep saturation region of the *B-H* curve can be approximately taken as a straight line, so

(8) $$f''[H_{DC}] = f'''[H_{DC}] = ... = 0,$$

Combining (6)-(8), we can reach:

(9) $$B_{AC}(t) = f'[H_{DC}]H_{AC}(t),$$

which means that $H_{AC}(t)$ and $B_{AC}(t)$ are in linear relationship.

As mentioned above, the AC magnetic field H_{AC} is not strictly sinusoidal due to the influence that the static permeability variation has on the AC leakage flux distribution. However, considering that the magnetic field generated by the DC superconducting coil is much larger than that generated by the AC coil, static permeability of the steel cores will not change much with the variation of the current in the AC coils. So the AC leakage flux changes little with AC excitation and can be ignored. So AC magnetic field H_{AC} is considered as sinusoidal.

Based on the above assumption that the model is linear, B_{AC} is also sinusoidal. So the problem becomes a sinusoidal steady one, and it can be solved by phasor method rather than by time-domain method.

To sum up, the simplified method is phasor calculation for linear model without DC coil. Equivalent permeability of the linear cores is taken as the slope of the deep saturation region of the *B-H* curve and the DC coil is removed. Magnetic field is solved by phasor method with only AC excitation. The AC flux or energy can be obtained easily by AC magnetic field calculation result and the inductance can then be solved. This method greatly reduces the complexity of the nonlinear time-domain solving process.

Actually, the deep saturation region of the *B-H* curve will not be given by material manufacturers. This is because that this region will not be widely used by normal electromagnetic devices, and additionally specialized measuring equipment will be required. Under normal circumstances, to solve the steady-state reactance of the SCSFCL or similar saturation problems, deep saturation region will have to be obtained by extending the most saturated section of the curve given by manufacturers in a linear way.

C. Static-Magnetic-Field Linear-Model Computation Method

Considering that the eddy current in the laminated steel cores and structure parts is small enough to be ignored in the reactance computation, the method to compute the magnetic field and then the reactance can be further simplified. It can be simplified as a static-magnetic-field linear-model solution.

Obviously, for a linear model without eddy current, its inductance is constant and unchanging with frequency. To compute such inductance, the solution of magnetic field with DC current is sufficient. Therefore, to compute the steady-state reactance of the SCSFCL, a DC current with arbitrary value can be added to AC coils and the magnetic field is computed. Afterwards, the inductance can be obtained from the magnetic energy, and the reactance can be obtained directly.

Computation example

An actual SCSFCL, as shown in Fig. 2, is simulated with the software ANSYS Maxwell by the three computing methods introduced above.

The parameters of this SCSFCL are shown in Table 1. And the B-H curve of its steel cores is shown in Fig. 5, where the deep saturation region has to be obtained by extending the most saturated section of curve given by manufacturers in a linear way, which will be a conservative design for the SCSFCL.

The steady-state reactance that are computed by the time-domain nonlinear model, the frequency-domain linear model and the static-magnetic-field linear model are shown in Table 2.

The flux waveform of the AC coils calculated by the time-domain nonlinear model is shown in Fig. 6 and the induced voltage of the AC coils is shown in Fig. 7. And the relative permeability distribution of the steel cores when the AC current is the largest value is demonstrated in Fig. 8.

Table 1. The parameters of an actual SCSFCL

	Items	Parameters
Cores	Material	Steel B30P105
	DC pillar diameter (mm)	916
	DC pillar height (mm)	2565
	AC pillar diameter (mm)	428
	AC pillar height (mm)	2565
	Yoke height (mm)	428
	Yoke thickness (mm)	428
	Window height (mm)	1191
	Window wideness (mm)	879
AC coil	Material	Copper
	Height (mm)	771
	Inner diameter (mm)	690
	Outer diameter (mm)	996
	Turns	25
	Current (kArms)	1.2
DC coil	Material	Superconductivity
	Height (mm)	643
	Inner diameter (mm)	1140
	Outer diameter (mm)	1168
	Excitation (kA* Turn)	421.2

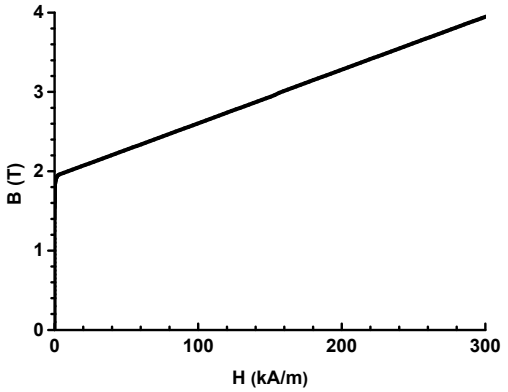

Fig. 5. B-H Curve of the steel cores.

Table 2 Computing result of reactance by three methods

Methods	Reactance (Ω)
time-domain nonlinear model	0.380
frequency-domain linear model	0.363
static-magnetic-field linear model	0.363

From Table 2, we can see that the computing result by the simplified method presented in this paper is almost the same with the result of the traditional time-domain nonlinear model. So the simplified method meets the requirement of the engineering, and it can be applied to the optimization calculation for the structure design of the SCSFCL, which will have a large amount of computation to do.

From Fig. 6 and Fig. 7, we can see that the waveform of both the induced voltage and the flux waveforms of the AC coils are approximately sinusoidal, which means that the relation between i_{AC} and H_{AC}, and the relation between H_{AC} and B_{AC} are both approximately linear.

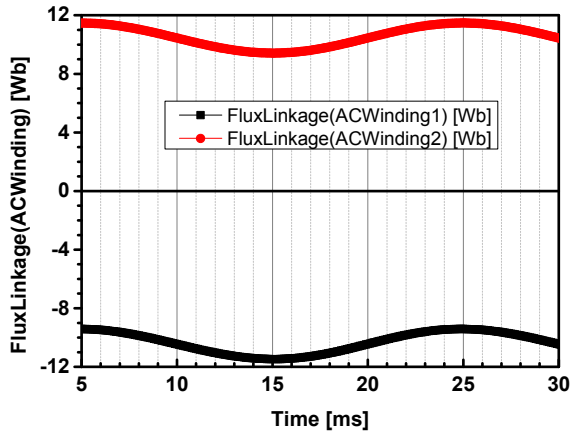

Fig. 6. Flux waveform of the AC winding.

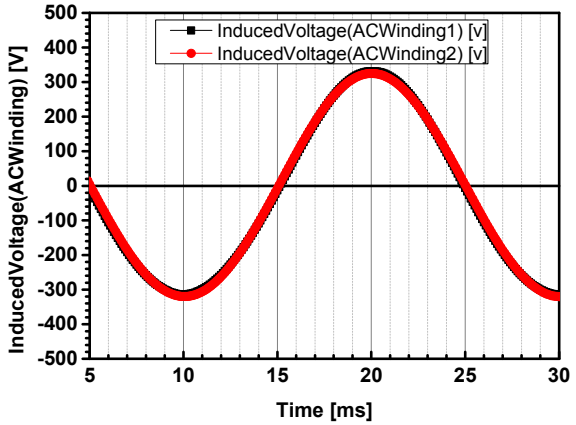

Fig. 7 Induced voltage waveform of the AC winding.

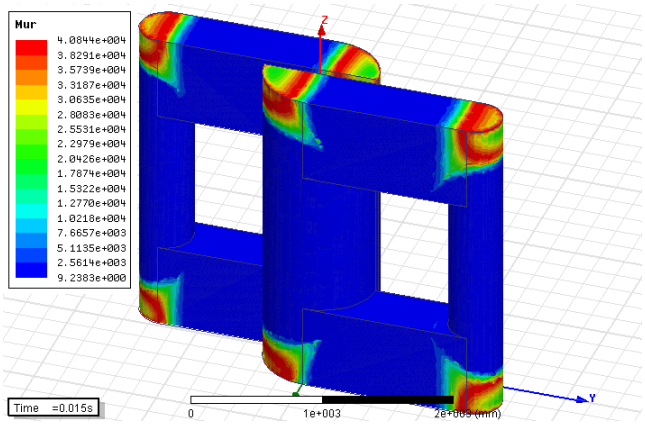

Fig. 8 The relative permeability distribution of the core.

From Fig. 8, we can see that although the AC current is the maximum value, the relative permeability of the steel cores is almost the same in the main path of the magnetic field. This is because the magnetic field generated by the DC coil is much larger than that generated by the AC coil. So the working state of the steel cores is barely influenced by the variation of the AC excitation.

Conclusions

1) It is not necessary to employ the nonlinear transient model to be simulated in time domain for the design computation of the steady-state reactance of the SCSFCL, which only means complexity, but not accuracy and no any good.

2) Considering that the deep saturation region of the *B-H* curve is approximately a straight line, the computation of the reactance can be simplified as a linear static-magnetic field solution, which can provide high enough accuracy.

3) No matter which model is adopted, the computation accuracy of the design reactance depends on the accuracy of the material B-H curve, especially in the deep saturation region. Therefore, it is an austere task to measure the B-H curve in deep saturation region to meet the design requirements of the SCSFCL. Currently, the capability of the measurement facility is not sufficient.

Acknowledgment

This project is supported by the National High-Tech R&D Program of China (863 Program, No. 2014AA032705).

***Authors**: Yuelong Jia, Tsinghua University, West Main Building 1-302, Tsinghua University, Beijing 100084 China, rhinestone@163.com,*
Li Hao, Tsinghua University, West Main Building 1-302, Tsinghua University, Beijing 100084 China, haol02@mails.tsinghua.edu.cn,
Zhengjun Shi, Guangdong Power Grid Corporation, Grid Planning & Research Centre, Guangdong Power Grid Corporation, Guangzhou 510600 China, shizhengjun@gd.csg.cn,
Haojun Zhu, Guangdong Power Grid Corporation, Grid Planning & Research Centre, Guangdong Power Grid Corporation, Guangzhou 510600 China, zhuhaojun@gd.csg.cn,
Jiansheng Yuan, Tsinghua University, West Main Building 1-302, Tsinghua University, Beijing 100084 China, yuan@tsinghua.edu.cn.

REFERENCES

[1] Y. Cai, S. Okuda, and et al., Study on Three-Phase Superconducting Fault Current Limiter, IEEE Trans. Appl. Supercond., 20 (2010), No. 3, pp. 1127-1130.

[2] L. Ye, M. Majoros, and et al., System Studies of the Superconducting Fault Current Limiter in Electrical Distribution Grids, IEEE Trans. Appl. Supercond, 17 (2007), No. 2, pp. 2339-2342.

[3] H. Kang, C. Lee, and et al., Development of a 13.2 kV/630 A (8.3 MVA) High Temperature Superconducting Fault Current Limiter, IEEE Trans. Appl. Supercond., 18 (2008), No. 2, 628-631.

[4] J. Cui, B. Shu, and et al., Safety Considerations in the Design, Fabrication, Testing, and Operation of the DC Bias Coil of a Saturated Iron-Core Superconducting Fault Current Limiter, IEEE Trans. Appl. Supercond. , 23 (2013), No. 3, 5600704.

[5] Y. Pan, M. Steurer, and et al., Impact of Waveform Distorting Fault Current Limiters on Previously Installed Overcurrent Relays, IEEE Trans. Power Delivery, 23 (2008), No. 3, 1310-1318.

[6] A. Abramovitz, K. Smedley, and et al., Prototyping and Testing of a 15 kV/1.2 kA Saturable Core HTS Fault Current Limiter, IEEE Trans. Power Delivery, 28 (2013), No. 3, 1271-1279.

[7] Y Nikulshin, Y Wolfus, and et al., Dynamic core length in saturated core fault current limiters, Superconductor Science and Technology, 26 (2013), No. 9, 095013.

[8] C. Zhao, S. Wang, and et al., Transient Simulation and Analysis for Saturated Core High Temperature Superconducting Fault Current Limiter, IEEE Trans. Magn., 43 (2002), No. 4, 1813-1816.